Available online at www.sciencedirect.com

SciVerse ScienceDirect

Journal of Nutritional Biochemistry 23 (2012) 1146–1154

Journal of Nutritional Biochemistry

Coordinate expression and localization of iron and zinc transporters explain iron–zinc interactions during uptake in Caco-2 cells: implications for iron uptake at the enterocyte☆

Vasuprada Iyengar, Raghu Pullakhandam, K. Madhavan Nair*

Micronutrient Research Group, National Institute of Nutrition, Indian Council of Medical Research, Jamai Osmania, Hyderabad 500 007, India

Received 25 October 2010; received in revised form 15 June 2011; accepted 27 June 2011

Abstract

Iron and zinc have diverse and important physiological functions. Yet, the mechanism of their absorption at the intestine remains controversial and is confounded by the fact that many studies have shown, to varying extents, that they inhibit the absorption of each other. We have studied the expression of iron and zinc transporters and storage proteins, and their regulation, in Caco-2 cells, an established enterocyte model, under normal culture conditions and under conditions of iron and zinc depletion and supplementation using a combination of immunoblotting, confocal microscopy and reverse transcriptase polymerase chain reaction. We show that divalent metal transporter-1 (DMT-1) delocalizes from the plasma membrane upon iron or zinc depletion, but its apical abundance increases with zinc supplementation. This translocation of DMT-1 coincides with an increase in iron uptake upon zinc supplementation, as previously reported by us. FPN-1 expression increases upon zinc supplementation and decreases with iron or zinc depletion, effluxing the excess sequestered iron and thus maintaining cellular iron homeostasis. Zinc influx transporters Zip-1 and Zip-14 and efflux transporters ZnT-1 and ZnT-4 are coordinately regulated under conditions of zinc supplementation and depletion to ensure cellular zinc homeostasis. We have previously reported that iron uptake can entail two transporters and that zinc noncompetitively inhibits iron uptake in Caco-2 cells. We now provide evidence that this inhibition is independent of DMT-1 and that Zip-14 may be a relevant iron transporter. These new observations provide experimental support to this two-transporter model of iron uptake and give mechanistic insight to iron–zinc interactions during uptake at the enterocyte.

Keywords: Caco-2 cells; DMT-1; FPN-1; Zip; ZnT; Iron–zinc interactions

1. Introduction

Iron and zinc are essential for growth, development and maintenance of physiological systems. Together, they play a major role in a wide variety of cellular functions that include proliferation and differentiation, oxidative metabolism and DNA synthesis. These, in turn, affect oxygen transport, hematopoiesis and the immune system.

It is now accepted that iron and zinc interact at the site of absorption, and interestingly, many combined iron–zinc supplementation trials in humans, including a recent meta-analysis, have reported varied efficacy [1–4], implying possible negative interactions. However, the mechanism and determinants of this interaction are not yet understood. Elucidating these interactions thus assumes importance because combined supplementation strategies are being formulated to simultaneously alleviate iron and zinc deficiencies.

Divalent metal transporter-1 (DMT-1) is the principal proton coupled metal–ion symporter for intestinal iron absorption [5, 6] and is regulated by cellular iron status [7]. Ferroportin-1 is the only known iron exporter and has been shown to be differentially regulated in a tissue-/cell-specific manner [8]. Cellular iron homeostasis therefore depends on these transporters, whose expression is controlled through the iron regulatory protein–iron responsive element (IRP-IRE) system which is exquisitely sensitive to perturbations in intracellular iron [9].

Zinc uptake in enterocytes occurs through the Zip family of transporters, and functional redundancy among Zip-1 and Zip-4 at the enterocyte is known (reviewed in Ref. [10]). Basolateral efflux into systemic circulation is accomplished principally by ZnT-1. The Zip and ZnT transporters are sensitive to alterations in zinc status and thought to be reciprocally regulated to maintain cellular zinc homeostasis [11]. Their expression has been shown to be transcriptionally regulated by the metal responsive element-binding transcription factor-1 [12], but posttranslational regulation has been shown for some Zip and ZnT transporters (reviewed in Ref. [10]). It is important to note that these observations are based on studies carried out with a variety of cells and do not necessarily operate in enterocytes.

☆ Sources of funding: the project is supported by a grant from the Department of Biotechnology, India (grant no. BT/PR/6728/AGR/02/334/2005). V.I. was supported by a fellowship from the University Grants Commission, Government of India.

* Corresponding author. Scientist-'E', Micronutrient Research, Biophysics Division, National Institute of Nutrition, Jamai Osmania, Hyderabad 500 007, India. Tel.: +91 40 27197269; fax: +91 40 27019074.

E-mail address: nairthayil@hotmail.com (K.M. Nair).

0955-2863/$ - see front matter © 2012 Elsevier Inc. All rights reserved.
doi:10.1016/j.jnutbio.2011.06.008

Several hypotheses have been postulated to explain iron–zinc interactions based on iron and zinc uptake studies in hepatocytes, oocytes and fibroblasts. It is possible that iron and zinc compete for the same influx transporter. DMT-1 has been shown to transport various divalent metal ions other than iron [13]. However, zinc transport through DMT-1 is still controversial [14,15]. By the same token, it is possible that there exists a zinc influx transporter capable of iron transport. Zip-2 and Zip-14 have been shown to be involved in systemic iron metabolism. Zip-14 has been shown to mediate non-transferrin-bound iron (NTBI) uptake [16], and Zip-2 knockout mice show deranged systemic iron metabolism [17]. Therefore, DMT-1, Zip-2 and Zip-14 are potential loci of iron–zinc interactions.

Recently, we have shown that zinc inhibits iron uptake, through mixed inhibition, in Caco-2 cells, an established model of absorptive enterocytes. Further, even acute changes in cellular zinc, but not those of iron, determine the nature of iron–zinc interactions [18]. Additionally, the expression of DMT-1 increased upon zinc supplementation, which coincided with increased iron uptake and the negation of zinc inhibition. To explain these observations, a two-transporter model of iron uptake was also proposed.

The aim of the present study was, therefore, to elucidate the role of iron and zinc transporters under conditions of acute, altered mineral status by analyzing their expression and localization, as these results can provide mechanistic insights into iron–zinc interactions during uptake.

2. Materials and methods

2.1. Materials

All chemicals were of tissue culture grade or the highest analytical grade available. All tissue culture ware was procured from M/s. Corning India Ltd. Unless otherwise specified, all chemicals were procured from M/s. Sigma-Aldrich, Bangalore, India. Desferroxamine (DFO) was obtained from M/s. Ciba, GmBH, Germany. Primary antibodies were procured either from M/s Santa Cruz Biotechnology Inc. (USA) or from M/s. Alpha diagnostic International (USA). All anti-species antibodies were procured from M/s. Sigma-Aldrich, Bangalore, India. Glass cover slips (19-mm diameter, English glass 1) and slides (75 mm×25 mm×1 mm) were procured locally from M/s. Bluestar.

3. Methods

3.1. Caco-2 cell culture

Caco-2 cells were obtained from the National Center for Cell Sciences (Pune, India), routinely maintained and used in experiments at passage 25–35. Cells were cultured in Dulbecco's modified Eagle's medium (DMEM) with 10% fetal bovine serum (FBS), 1% NEAA (non-essential amino acids), 0.4 mM glutamine and 1% antibiotic–antimycotic solution. Cells were seeded at a density of 50,000 cells/cm^2 and maintained at 37°C in an incubator with a 5% CO_2/95% air atmosphere at constant humidity. Cells were passaged at 3-day intervals at 70% confluency and used for experiments at 11–13 days postconfluency.

3.2. Experimental design

Caco-2 cells were grown and maintained in six-well plates and were iron or zinc depleted or supplemented as given below. Cells in fresh DMEM were supplemented with 50 μM iron or zinc (as respective sulfate salts) for a period of 3 h. Cells in fresh DMEM were depleted of iron using 100 μM DFO for 8 h or depleted of zinc using 10 μM *N*,*N*,*N*′,*N*′-teterakis [2-pyridylmethyl] ethylene diamine (TPEN) for 3 h. Depletion and supplementation were carried out simultaneously in separate sets of cells. Cells in DMEM alone served as control cells. Optimization of time and concentration of DFO, TPEN and minerals, either alone or in combination, were performed as mentioned elsewhere [18]. Under these conditions, iron and zinc uptakes, using radioisotopes, both individually and in an equimolar ratio combination, have been reported by us earlier [18].

Table 1
List of antibodies used and their concentrations

Antibody against	Primary antibody		Anti-species antibody	
	Dilution	Raised in	Dilution	Raised in
DMT-1	1:500 (SC); 1:1000 (ADI)	Rabbit	1:2000	Goat
IRP-1	1:250 (SC)	Rabbit	1:2000	Goat
IRP-2	1:1000 (ADI)	Mouse	1:2000	Rabbit
FPN-1	1:1000 (ADI)	Rabbit	1:2000	Goat
ZnT-1	1:1000 (SC)	Goat	1:1000	Rabbit
ZnT-4	1:1000 (SC)	Goat	1:1000	Rabbit
hrMT-2	1:1000 (in-house antiserum)	Rabbit	1:2000	Goat
GAPDH	1:1000 (SC)	Rabbit	1:2000	Goat
Villin	1:1000 (SC)	Rabbit	1:2000	Goat

ADI, Alpha Diagnostic Intl.; SC, Santa Cruz Biotechnology Inc.

3.3. Immunoblotting for proteins

Cells (in six-well plates) in fresh DMEM (2 ml/well) were left untreated (control) and incubated with iron, zinc, TPEN or DFO. After incubation, the spent medium was discarded; cells were washed in ice-cold phosphate-buffered saline (PBS), lysed and subjected to immunoblotting for FPN-1, IRP-1, IRP-2, MT, ZnT-1 and ZnT-4 as follows. GAPDH was used to ensure equal loading of proteins.

About 60 μg of protein was resolved on 10% sodium dodecyl sulfate polyacrylamide gels [19], electrotransferred (MiniProtean, Bio-Rad, Hercules, CA, USA) on to nitrocellulose membrane, blocked with 3% nonfat dry milk and incubated with the primary antibodies overnight at 4°C followed by horseradish-peroxidase-conjugated anti-species antibody (according to the manufacturer's instructions, Table 1). Bands were visualized using the TMB substrate system, scanned in a GS-710 densitometric scanner and quantitated using Quantity-one software (Bio-Rad, Hercules, CA, USA).

IRP-1 and IRP-2 expression, after the incubations, was studied in the microsomal fraction isolated from cells grown in T-75 flasks (10 ml DMEM per flask during the above-mentioned incubations)[20] and was prepared as follows. Cells were washed in ice-cold PBS and scraped into 3 ml of digitonin buffer (20 mM Tris–Cl, pH 7.4; 250 mM sucrose; 0.007% digitonin; 5% 1× protease inhibitor cocktail) per flask. Cells were manually homogenized using 21G and $26_{1/2}$ G needles and kept on ice for 15 min with intermittent vortexing. The homogenate was centrifuged at 1500*g* for 10 min, and the pellet was discarded. The supernatant was centrifuged at 10,000*g* for 10 min, and the pellet was labeled as the membrane fraction and kept on ice. The supernatant was further ultracentrifuged at 100,000*g* for 60 min. The pellet was labeled cytosolic precipitate. The supernatant was labeled as soluble cytosolic preparation and contains the free form of IRP-1. The pellets from the 10,000*g* and 100,000*g* were pooled in TX-100 buffer (20 mM Tris–Cl, pH 7.4; 250 mM sucrose; 1% TX-100; 5% protease inhibitor cocktail), dissolved by vortexing and labeled as cytosolic precipitate, and this fraction contains the RNA-bound form. Both the cytosolic precipitate and the soluble cytosolic preparation were then subjected to Western blotting for IRP-1 and IRP-2 proteins as above. Villin was used to ensure equal loading of the cytosolic precipitate.

3.4. Western blotting for MT

The following changes were made from the above-mentioned procedure and are according to the method of Yasunobu and Suzuki [21]. Samples were boiled in a buffer that did not contain any

reducing agent and had 0.25 mg/ml Cd. Samples were electrophoresed as mentioned above and electrotransferred at 30 mA overnight at 25°C. Immunodetection of MT was done as for all other proteins using an in-house antiserum raised against rhMT 1 [22].

3.5. Estimation of aconitase activity

Briefly, approximately 1×10^6 cells were homogenized in 100 μl of assay buffer provided and centrifuged at 800*g* for 10 min at 4°C, the supernatant was collected, and protein was estimated using the BCA kit. Aconitase activity was measured spectrophotometrically in a microplate reader (Bio-Tek instruments Ltd.) at 450 nm in a 96-well microplate format using a kit (M/s. Biovision Research Products, USA). Enzyme activity in mU (nmol/min/mg protein) was calculated from an isocitrate standard curve run simultaneously with the samples. One unit of enzyme isomerizes 1.0 μmol of citrate to isocitrate per min at pH 7.4 at 25°C.

3.6. Estimation of ferritin by enzyme-linked immunosorbent assay (ELISA)

Ferritin was estimated by a ELISA method developed and validated in-house [23].

3.7. Reverse transcription polymerase chain reaction (RT–PCR)

After the incubations, cells in T-75 flasks were processed for RNA isolation and semiquantitative RT-PCR as follows. Total RNA was isolated from cells using the TRIzol reagent (M/s. Sigma-Aldrich) as per the manufacturer's protocol. The reverse transcription reaction was performed (20 μl), after equalizing total RNA, in an Eppendorf Mastercycler PCR instrument. Primers were designed (Table 2) using Primer 3.0 software (ver. 0.4.0) and custom synthesized (M/s Ocimum Biosciences, Hyderabad). The PCR of 20-μl volume was set up, and conditions were optimized for each gene of interest (Table 2). The amplified products were run on 1.5% agarose gel at 100 V. The image was acquired in a gel doc system (Bio-Rad) under UV illumination, and relative band intensity was quantitated using Quantity One software (Bio-Rad).

3.8. Confocal microscopy for transporter localization

Cells for confocal experiments were seeded at a density of 50,000 cells/cm^2 on presterilized circular cover slips in 12-well plates. Cells in fresh DMEM were left untreated (control) or incubated with iron, zinc, TPEN and DFO. After experiment(s), medium was aspirated, and all subsequent procedures were carried out with mild shaking.

3.8.1. Fixing and preparation of cells

All volumes are for a single well. Cells were washed twice with 500 μl of ice-cold 1× PBS, fixed with 450 μl of formaldehyde solution (4% formaldehyde in PBS, prepared just prior to use) and incubated at RT for 20 min. The solution was thoroughly aspirated, and cells were washed (thrice, 400 μl of 0.1% Tween-20, 100 mM glycine in 1× PBS), permeabilized on ice for 5 min (500 μl of 0.2% Triton X-100 in 1× PBS), blocked (500 μl of 5% FBS in 1× PBS) for 20 min at RT and washed. A total of 150 μl of 1:100 diluted (in 50 mM TBST) primary antibody (DMT-1/ZnT-1/ZnT-4) was incubated for 1 h at 37°C, washed thrice with TBST, incubated with 150 μl of 1:1000 diluted (50 mM TBST) FITC-labeled anti-species antibody for 1 h at 37°C and washed thrice with TBST. Cells on cover glass were mounted using 8 μl of mounting media [49% 1× PBS, 49% glycerol, 2% n-propyl gallate (wt/vol), 1 μL/ml DAPI (4',6-diamidino-2-phenylindole)], and the edges were sealed using transparent nail varnish. These were subsequently viewed in a confocal laser scanning microscope.

3.8.2. Confocal acquisition parameters and image analyses

Fluorescence was observed and quantified using a Leica SP5 AOBS laser scanning confocal microscope under 63× oil immersion lens. For all samples, the acquisition parameters were the same and are as follows. Cell height was adjusted to approximately 20 μm; pinhole size was set at 67.94 with *z*-magnification of 8.16; laser power was set at 20% for both FICT (fluorescein isothiocyanate) and DAPI with PMT (photomultiplier tube) gain of 1039 V for FITC and 775 V for DAPI, and 100 stacks were acquired per image. All other parameters were kept at default settings to maintain uniformity across acquisitions. A stack profile was built, and a full report was generated for each sample which also contained the maximum projection image. All analyses were performed using the LASAF-lite software, ver. 1.8.2 build 1465.

3.9. Statistical analyses

All protein expression, confocal, RT-PCR experiments were performed thrice to generate three independent observations. Data are presented as mean±S.D. Means between groups or between time points within a group were compared by one-way analysis of variance and post hoc *t* test (SPSS software, version 11.0). $P<.05$ was considered significant.

4. Results

No significant changes in ferritin levels were observed with iron or zinc depletion or supplementation (Fig. 1A). Zinc supplementation, on the other hand, significantly increased MT expression, and DFO significantly decreased MT expression. TPEN treatment also tended to decrease MT levels (Fig. 1B).

Apical DMT-1 fluorescence increased upon zinc supplementation compared to untreated cells. However, iron (DFO) or zinc (TPEN) depletion resulted in marked delocalization of DMT-1 fluorescence away from the apical surface and accumulated towards the center of the cell, as evidenced by a shift in the cell height at maximum amplitude (Fig. 2A, graph). Iron supplementation did not have any significant effect on the localization of DMT-1. Expression of FPN-1 increased upon supplementation with iron or zinc and upon depletion of zinc and did not change with DFO (Fig. 2B).

Total cellular IRP-1 protein expression did not change upon supplementation or depletion of iron and zinc (Fig. 3A). The RNA-bound form decreased upon iron supplementation but significantly

Table 2
Primer sequences and PCR conditions

Gene	NLM ID	Forward primer	Reverse primer	Amp size (bp)
Zip-1	NM_014437.3	TCCCAAGGAACAAGAGATGG	CTGAAATGGGCTAGGACCAA	213
Zip-14	NM_015359.2	GCAGCTTCGACCTCATTTTC	CGCTACCCAAACAGAGAAGC	246
β-Actin	NM_001101.3	CTCTTCCAGCCTTCCTTCCT	CACCTTCACCGTTCCAGTTT	511

PCR conditions: denaturation 94°C, 60 s; annealing 56°C, 45 s; elongation 70°C, 60 s; 30 cycles for Zip-1/Zip14, 25 cycles for β-actin.

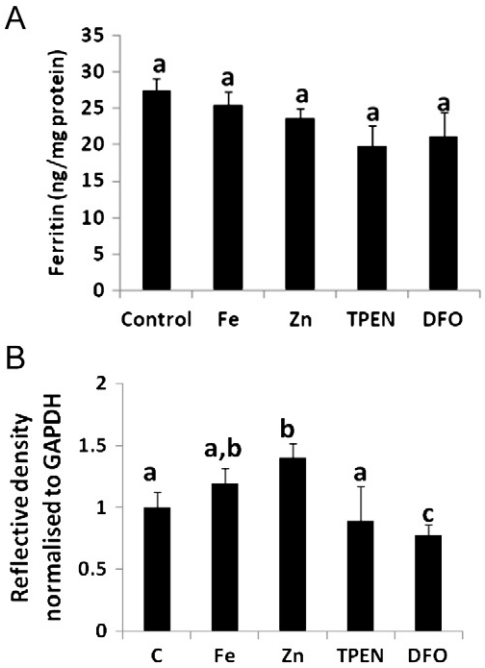

Fig. 1. Effect of iron and zinc depletion or supplementation on ferritin and MT. Cells were left untreated (control, C) or depleted or supplemented with iron or zinc. Ferritin (A) was estimated by a sandwich ELISA (n=6), and metallothionein (B) expression was quantitated from an immunoblot (n=3, not shown). Results are mean±S.D. Bars that do not share a common superscript are significantly different at P<.05.

increased upon zinc supplementation compared to control (Fig. 3B). Chelation of cellular iron and zinc also increased the bound form. The cytosolic form increased with iron supplementation but decreased upon zinc supplementation and depletion of iron and zinc compared to controls (Fig. 3B). Aconitase activity was reduced with iron and zinc supplementation, but remained unaltered upon depletion of either iron or zinc. Zinc supplementation increased IRP-2 expression; however, iron supplementation or depletion with DFO and TPEN did not alter IRP-2 expression (Fig. 3D).

Transcript levels of Zip-1 and Zip-14 significantly increased upon zinc depletion with TPEN. Interestingly, Zip-14 transcript level alone decreased with zinc supplementation, with no change in Zip-1 transcript levels (Fig. 4).

Supplementation with iron and zinc significantly increased ZnT-1 expression; the increase with zinc supplementation was higher when compared with iron supplementation. TPEN and DFO also significantly increased ZnT-1 expression (Fig. 5). Supplementation with zinc and depletion with TPEN and DFO did not significantly affect ZnT-4 expression compared to untreated cells (Fig. 5).

No significant changes in ZnT-1 localization (cell height at maximum amplitude) were observed except for diffuse punctate fluorescence upon zinc supplementation which was markedly enhanced upon zinc depletion with TPEN (Fig. 6A).

Zinc supplementation resulted in marked increase in discrete punctate ZnT-4 fluorescence; TPEN and DFO also resulted in punctate fluorescence of ZnT-4, but this was relatively lesser than that observed with zinc supplementation. No significant differences in localization (cell height at maximum amplitude) were observed (Fig. 6B).

5. Discussion

Systemic iron and zinc homeostasis is the resultant of exquisitely coordinated processes, with the enterocyte playing a major role. Given the similarities in the physicochemical properties between iron and zinc, it is not surprising that these trace metals influence the transport of one another across the enterocyte. However, precious little is known about the mechanisms that mediate these interactions. We have previously proposed a model of iron uptake that entailed two transporters for iron, one of which is DMT-1 and the other an "unknown" transporter which could be primarily a zinc transporter [18]. The results reported herein are aimed at understanding the role of the iron and zinc transport proteins in iron–zinc interactions and to provide a mechanistic basis for the interactions and, in effect, also verify the proposed model.

That acute depletion and supplementation effectively and desirably altered cellular iron and zinc status is evidenced by a decrease in metallothionein and ferritin during depletion and by their increase during supplementation. Having previously established that zinc supplementation increases DMT-1 expression [18], confocal microscopy was used to pinpoint the cellular distribution of DMT-1 after acute cellular iron or zinc depletion or supplementation. The increased apical localization of DMT-1 upon zinc supplementation implies that the enhanced iron uptake reported previously [18] was indeed DMT-1 mediated. However, as excess iron is deleterious to cells, it is probably effluxed through FPN-1, whose expression also concurrently increased upon zinc supplementation. These results suggest that zinc-supplemented cells not only take up more iron but also transfer the excess iron out of the cell, underscoring the importance of cellular zinc status in determining iron uptake and iron–zinc interactions during uptake. This is substantiated by the fact that there was no significant increase in cellular ferritin levels upon zinc supplementation.

FPN-1 expression also increased upon iron supplementation, which probably led to maintenance of cellular iron homeostasis, as there was no net change in ferritin. The marked relocalization of DMT-1 away from the apical surface of the cell upon treatment with TPEN and DFO, in spite of no change in total DMT-1 expression, explains the previously reported decrease in iron uptake due to depletion of zinc (TPEN) or iron (DFO) [18]. In partial agreement with our results, cytoplasmic staining of DMT-1 has been shown in enterocytes of iron-deficient subjects [24].

Importantly, these changes observed in the cellular distribution of DMT-1 imply that DMT-1 is not the site of negative interactions between iron and zinc during uptake. This implication is explained as follows. We have previously shown that zinc supplementation increases iron uptake and abrogates negative interactions between iron and zinc [18]. If DMT-1 was simultaneously transporting iron and zinc, increased apical DMT-1 localization, upon zinc supplementation, should result in persistent zinc inhibition of iron uptake, but we have observed abrogation of the negative interactions. Moreover, TPEN and DFO treatment resulted in the redistribution of DMT-1 away from the apical surface of the cell and was accompanied by an increase in zinc uptake rather than a decrease. Similar observations that DMT-1 may not be a physiologically relevant zinc transporter have been reported by others [14,15].

Zinc depletion also led to increased FPN-1, the reason for which is not known. However, given the ability of zinc to inhibit iron-exasperated oxidative signaling [22], it is probable that the acute decrease in cellular zinc signals a need to reduce free iron (the labile iron pool) within the cell. This would minimize incident oxidant-induced damage. Taken together, these results show that there is coordinate regulation of DMT-1 and FPN-1 to ensure efficient uptake and transfer of acquired iron to basolateral circulation without the retention of excess iron. This is in agreement with the conclusions reached by Zoller et al. [25], who also show coordinate regulation of duodenal DMT-1 and FPN-1 in iron deficiency and iron overload. However, the zinc status of these subjects is not known.

In order to explain the changes in DMT-1 and FPN-1 expression, changes in IRPs were also assessed. Iron supplementation decreased

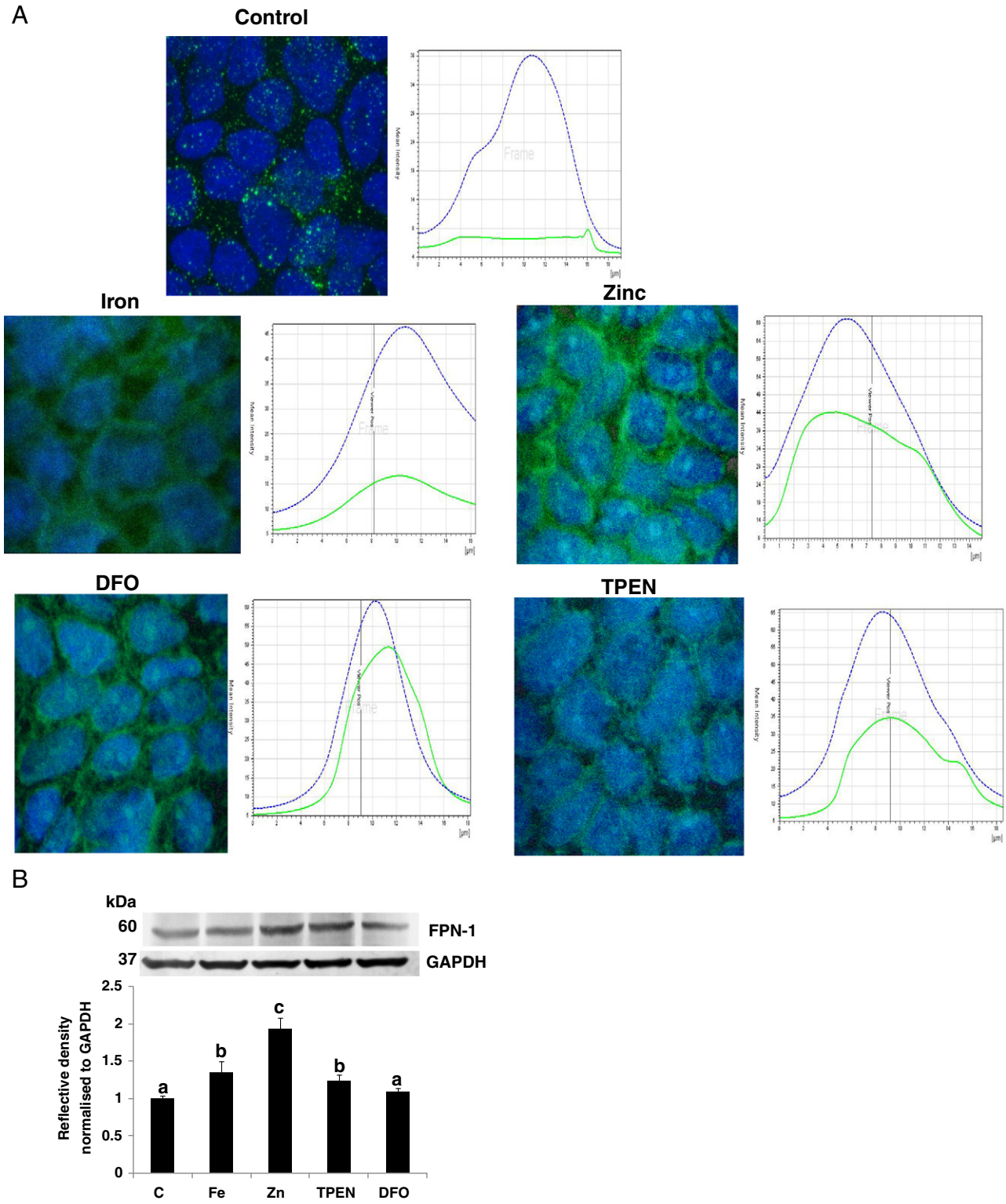

Fig. 2. Effect of depletion or supplementation on intracellular DMT-1 localization and FPN-1 expression in control cells or in the presence of 50 μM iron, 50 μM zinc, 10 μM TPEN or 100 μM DFO. (A) Confocal microscopy images of DMT-1 at maximum fluorescence. Intracellular DMT-1 (green) distribution upon iron–zinc depletion–supplementation, with nucleus stained with DAPI (blue). Images were acquired in triplicate ($n=3$), and a representative image is shown. The accompanying graph is the stack profile of the image. (B) Immunoblot of FPN-1 protein. Cells were left untreated (C), supplemented with 50 μM Zn/50 μM Fe, zinc depleted with 10 μM TPEN (TPEN), iron depleted with 100 μM DFO (DFO). Bar graph represents FPN-1 band reflective density normalized to respective GAPDH intensities. Bars with different superscripts are significantly different at $P<.05$. Immunoblots were repeated at least twice ($n=3$), and representative blots are shown.

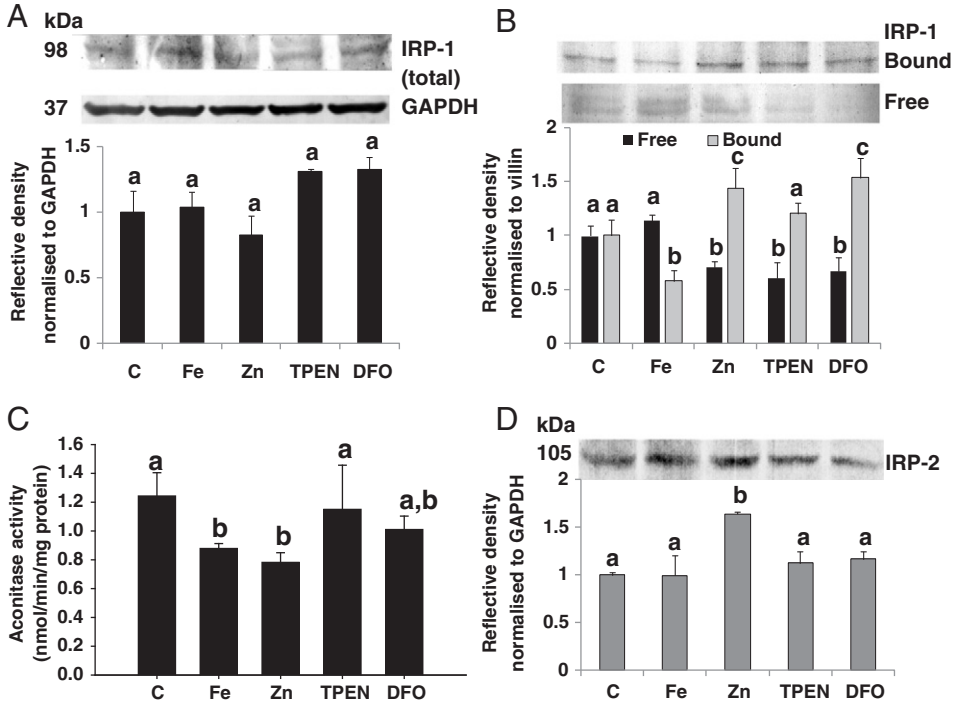

Fig. 3. Effect of depletion or supplementation on IRP-1 protein expression. Cells were left untreated (C), supplemented with 50 μM Zn/50 μM Fe, zinc depleted with 10 μM TPEN (TPEN), iron depleted with 100 μM DFO (DFO). Total IRP-1 protein expression (A), RNA-bound and cytosolic free form of IRP-1 (B) with reflective density normalized to GAPDH and aconitase enzyme activity (C) and immunoblot of IRP-2 protein (D). Bar graphs are mean±S.D. Bars with different superscripts are significantly different at $P<.05$. Immunoblots were repeated at least twice ($n=3$), and representative blots are shown.

the bound form but increased the free form of IRP-1, while iron depletion (DFO) increased the bound form of IRP-1 without altering total IRP-1 protein levels. Thus, the IRP-IRE system was sensitive to acute changes in cellular iron concentrations under the present experimental conditions, as has been reported previously [20]. Of greater interest though is the fact that zinc supplementation increased both the RNA-bound form of IRP-1 and IRP-2 expression, resulting in increased DMT-1. This implies that the observed changes in DMT-1 expression upon zinc supplementation are under the control of the IRP-IRE system. Further, zinc supplementation inhibited aconitase activity, probably as it enhanced the RNA-bound form, given that total IRP-1 protein levels did not change. In concurrence,

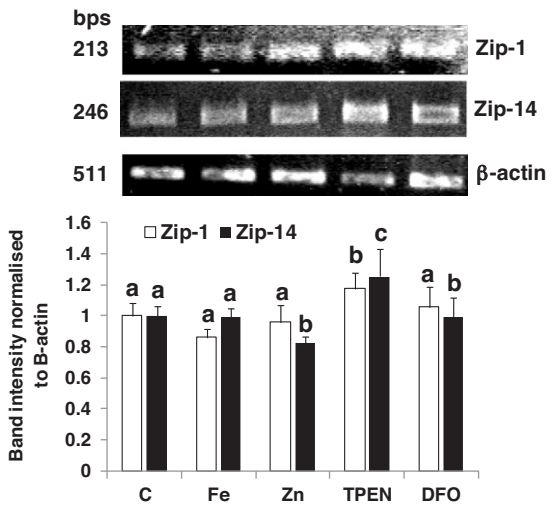

Fig. 4. Effect of depletion or supplementation on Zip transporter transcript level. RT-PCR of Zip-1 and Zip-14 transporter mRNA levels. Cells were left untreated (C), supplemented with 50 μM Zn/50 μM Fe, zinc depleted with 10 μM TPEN (TPEN), iron depleted with 100 μM DFO (DFO). Bar graph represents DNA band intensity normalized to respective β-actin intensities. Bars with different superscripts are significantly different at $P<.05$. PCRs were repeated at least twice ($n=6$), and representative gels are shown.

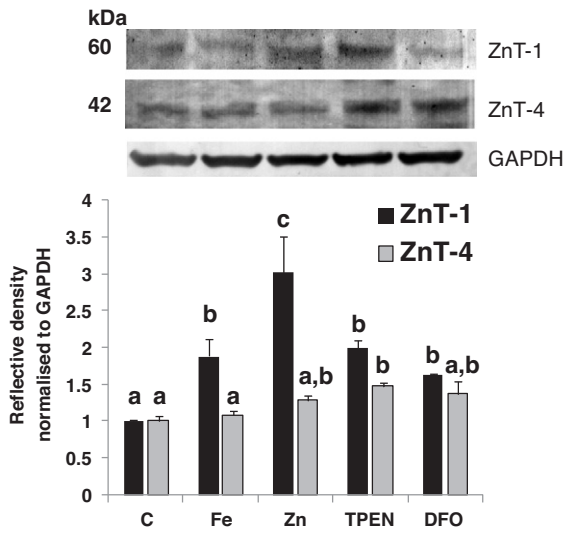

Fig. 5. Effect of depletion or supplementation on ZnT transporter expression. Immunoblot of ZnT-1 (dark bars), ZnT-4 (light bars) proteins. Cells were left untreated (C), supplemented with 50 μM Zn/50 μM Fe, zinc depleted with 10 μM TPEN (TPEN), iron depleted with 100 μM DFO (DFO). Bar graph represents protein band reflective density normalized to respective GAPDH intensities. Bars with different superscripts are significantly different at $P<.05$. Immunoblots were repeated at least twice ($n=3$), and representative blots are shown.

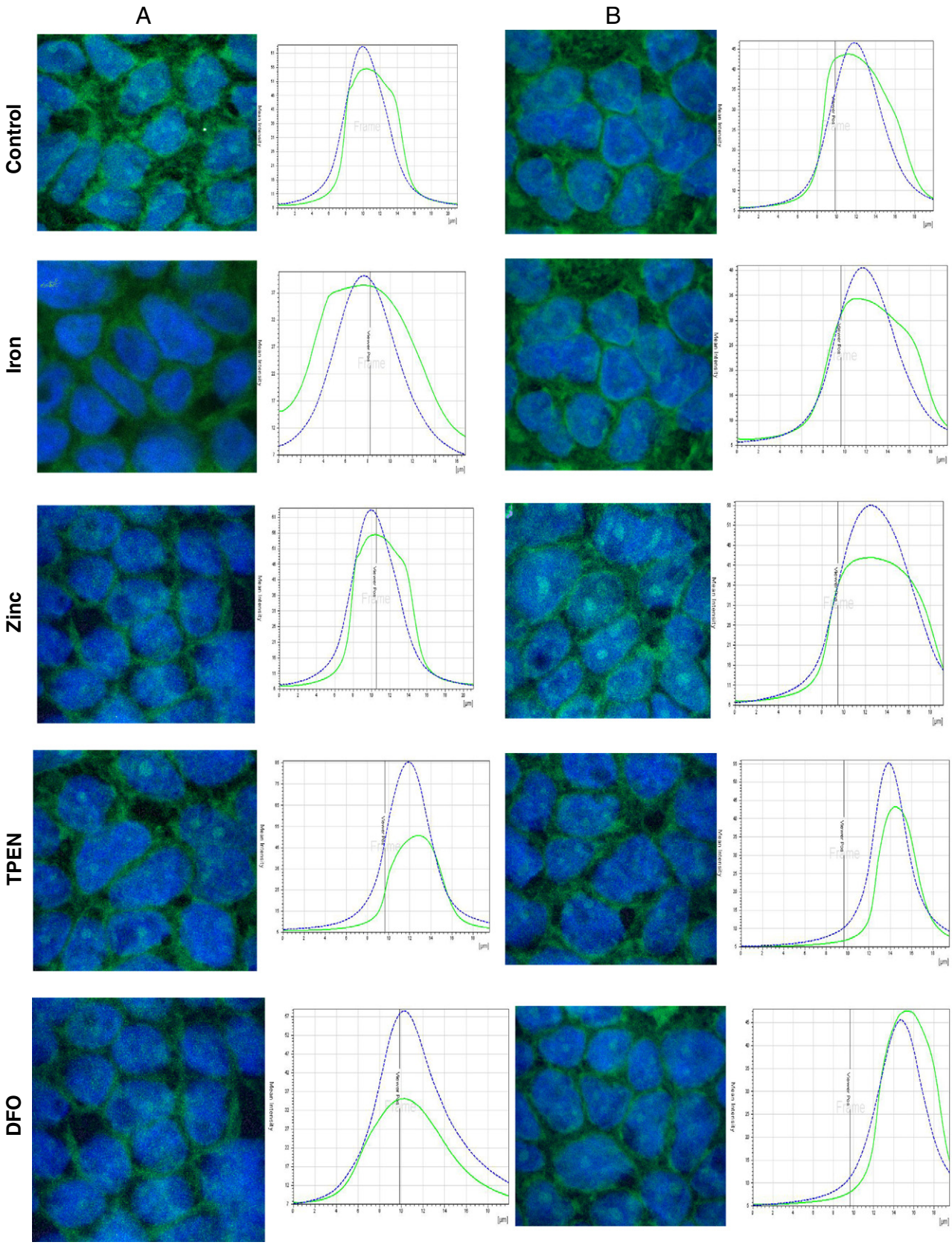

Fig. 6. Effect of depletion or supplementation on intracellular ZnT-1, ZnT-4 localization in control cells, or supplemented with 50 μM iron, 50 μM zinc, 10 μM TPEN or 100 μM DFO. Confocal microscopy images of ZnT-1 (A) and ZnT-4 (B) at maximum fluorescence. Intracellular ZnT-1 or ZnT-4 (green) distribution upon iron–zinc depletion–supplementation, with nucleus stained with DAPI (blue). Graphs are the stack profile of the images. Images were acquired in triplicate ($n=3$), and a representative image is shown.

previously, studies from this laboratory have reported that zinc inhibits aconitase and that aconitase activity is a sensitive marker of iron–zinc interactions during absorption in the rat model [26].

It is intriguing to note, however, that the FPN-1 transcript IRE is present in the 5′UTR and activation of IRP binding should lead to decreased FPN-1 expression. However, we observed an increase, implying that FPN-1 may not be under the control of the IRP-IRE system. This is consistent with earlier published results and reports of increase in FPN-1 transcript and protein in enterocytes under conditions of iron deficiency in both mice and humans, presumably involving both transcriptional and posttranslational regulation [8,24]. It is tempting to postulate that this increase in FPN-1 expression, in response to iron deficiency, may serve to enhance basolateral iron transfer to systemic circulation, thus narrowing the gap between iron supply and demand.

We have previously shown that significant changes in zinc uptake, whether in the presence or absence of concomitant equimolar iron, occurred only upon zinc depletion; zinc supplementation had no significant effect [18]. One of the limitations of the current study is that we have studied only selected transporters rather than screening all known Zip and ZnT proteins. Therefore, it is important to mention here that we used Zip-1 as a representative of Zip transporters in Caco-2 cells, while our interest in Zip-14 lies in the fact that it has been shown to mediate NTBI uptake in hepatocytes [16]. We did not look at Zip-4 expression because it has been shown earlier that Zip-4 mRNA levels are not significantly altered in response to acute changes in cellular zinc status in Caco-2 cells [27] apart from the fact that it is a specific zinc transporter that cannot transport other metals such as iron [28]. In accordance with previously reported changes in zinc uptake, Zip-1 and Zip-14 mRNA levels increased with TPEN. It is interesting that zinc supplementation (for 3 h) significantly decreased only Zip-14 transcript levels but not Zip-1, implying that Zip-14 in Caco-2 cells is probably more sensitive to acute changes in cellular zinc status. The fact that significant changes in Zip-1 mRNA were not observed upon short duration of zinc supplementation is in conformance with other reports of Zip-1 being refractory to excess zinc in mice, but sensitive to only zinc deficiency (reviewed in Ref. [10]).

Zinc supplementation significantly increased ZnT-1 expression, as did iron supplementation; TPEN and DFO treatments and confocal microscopy showed diffuse punctate fluorescence. The increased ZnT-1 expression upon zinc supplementation would result in the efflux of the zinc taken up due to zinc supplementation, resulting in maintenance of cellular zinc status. Iron-supplementation-induced increase in ZnT-1 probably serves to maintain cellular zinc homeostasis given that we have previously shown that concomitant equimolar iron increases zinc uptake [18]. The diffuse punctate fluorescence implies that ZnT-1 has localized to vesicles.

ZnT-4 expression increased significantly only with TPEN and was accompanied by diffuse punctate fluorescence throughout the cell, as visualized by confocal immunolocalization. Zinc supplementation did not significantly increase ZnT-4 expression but resulted in strong punctate fluorescence throughout the cell, probably corresponding to zinc-loaded endosomes or vesicles, “zincosomes” [29]. This is consistent with reported results that ZnT-4 mediates excess cytosolic zinc sequestration into endosomes [30]. Iron supplementation did not alter ZnT-4 expression or localization. DFO did not alter ZnT-4 expression, but the pattern of localization was similar to that of TPEN, i.e., diffuse punctate fluorescence throughout the cell, indicating that the observed punctate fluorescence is probably due to partial chelation of zinc rather than iron depletion as DFO can chelate zinc to a certain extent [31].

The magnitude of changes in protein expression with zinc depletion or supplementation was greater in ZnT-1 than in ZnT-4 and is in agreement with reports of ZnT-4 expression being refractory to zinc depletion–supplementation. Instead, localization data show that there is increased intracellular trafficking of the protein between the Golgi and endosomal vesicles (reviewed in Refs. [10,32]). These changes in ZnT-1 and ZnT-4 are similar, and both localize to intracellular vesicles upon cytosolic zinc chelation. In keeping with the general function of ZnT transporters, it is logical to expect that ZnT-1 and ZnT-4 expression should decrease upon zinc chelation, but our results show an increase. It has been previously shown that both ZnT-1 and ZnT-4 can localize equally to both apical and basolateral vesicles in response to changes in zinc status, and this may enable zinc acquisition at the plasma membrane in response to decreased cellular zinc [11,33,34]. A similar mechanism may be operational here. Also, it is possible that once cellular zinc levels have been restored, ZnT-1 expression level will return to baseline levels. The results presented herein also lead to the inference that changes in cellular iron concentration did not significantly affect zinc transport proteins. This is completely contrary to the substantial effects of zinc supplementation or depletion on iron transporters and the IRPs.

Finally, the changes observed with localization of DMT-1 and expression of Zip-1 and Zip-14 transcripts can clearly explain the two-transporter model that we have proposed earlier [18] (Supplementary Figure 1). There are two transporters capable of iron transport, of which DMT-1 is already established. Based on our previous results and the data presented here, it is possible that Zip-14 is a candidate for the predicted putative iron transporter, especially because its expression is reciprocally and acutely modulated by cellular zinc status. Further, Zip-14 has been shown to transport NTBI along with zinc [16]. Under the present experimental conditions, there was no decrease in Zip-1 levels, which precludes its consideration as a candidate iron transporter. Zip-2 is not expressed in Caco-2 cells, although it is important in liver iron homeostasis and during murine embryo development [17]. While extensive experimentation will be needed to conclusively prove that Zip-14 is indeed the “other” iron transporter, the present results are encouraging and warrant further investigation.

6. Conclusions

The above results, for the first time, mechanistically explain iron–zinc interactions at the transporter level. DMT-1 cannot be the site of negative interactions between iron and zinc. Zip-14 seems an ideal candidate as the “other” iron transporter that can transport both iron and zinc and therefore be the site of interactions between iron and zinc. Cellular zinc dictates the course of events that determine the expression of proteins involved in cellular iron metabolism; a vice-versa effect of iron is conspicuously absent. The reason for such predominance of cellular zinc status as a determinant of iron–zinc interactions and the mechanism by which zinc brings about these changes are currently not known, but may be due to zinc-induced changes in the cellular labile iron pool.

Supplementary materials related to this article can be found online at doi:10.1016/j.jnutbio.2011.06.008.

Acknowledgments

FITC-conjugated anti-species antibodies were a kind gift from Prof. Manjula Sritharan, School of Life Sciences, Hyderabad Central University, Hyderabad.

References

[1] Solomons NW, Pineda O, Viteri F, Sandstead HH. Studies on the bioavailability of zinc in humans: mechanism of the intestinal interaction of non-heme iron and zinc. J Nutr 1983;113(2):337–49.

[2] Whittaker P. Iron and zinc interactions in humans. Am J Clin Nutr 1998;68: 442S–6S.
[3] Lind T, Lonnerdal B, Stenlund H, Ismail D, Seswandhana R, Ekstrom E, et al. A community-based randomized controlled trial of iron and zinc supplementation in Indonesian infants: interactions between iron and zinc. Am J Clin Nutr 2003;77: 883–90.
[4] Wieringa FT, Berger J, Dijkhuizen MA, Hidayat A, Ninh NX, Utomo B, et al, for the SEAMTIZI. Combined iron and zinc supplementation in infants improved iron and zinc status, but interactions reduced efficacy in a multi-country trial in Southeast Asia. J Nutr 2007;137:466–71.
[5] Gunshin H, Mackenzie B, Berger UV, Gunshin Y, Romero MF, Boron WF, Nussberger S, Gollan JL, Hediger MA. Cloning and characterization of a mammalian proton-coupled metal–ion transporter. Nature 1997;388:482–8.
[6] Mackenzie B, Hediger MA. SLC-11 family of H^+-coupled metal–ion transporters NRAMP-1 and DMT-1. Eur J Physiol 2004;447:571–9.
[7] Mackenzie B, Garrick MD, Iron Imports II. Iron uptake at the apical membrane in the intestine. Am J Physiol Gastrointest Liver Physiol 2005;289:G981–6.
[8] McKie AT, Marciani P, Rolfs A, Brennan K, et al. A novel duodenal iron-regulated transporter, IREG1, implicated in the basolateral transfer of iron to the circulation. Mol Cell 2000;5:299–309.
[9] Pantopoulous K. Iron metabolism and the IRE/IRP regulatory system. Ann N Y Acad Sci 2004;1012:1–13.
[10] Litchen LA, Cousins RJ. Mammalian zinc transporters — nutritional and physiologic regulation. Ann Rev Nutr 2009;29:133–52.
[11] Cousins RJ, Liuzzi JP, Lichten LA. Mammalian zinc transport, trafficking, and signals. J Biol Chem 2006;281(34):24085–9.
[12] Laity JH, Andrews GK. Understanding the mechanisms of zinc-sensing by metal-response element binding transcription factor-1 (MTF-1). Arch Biochem Biophys 2007;463:201–10.
[13] Sacher A, Cohen A, Nelson N. Properties of the mammalian and yeast metal–ion transporters Dct1 and smf1p expressed in xenopus laevis oocytes. J Exp Biol 2001;204:1053–61.
[14] Mackenzie B, Takanaga H, Hubert N, Rolfs A, Hediger MA. Functional properties of multiple isoforms of the human divalent metal–ion transporter DMT-1. Biochem J 2007;403:59–69.
[15] Garrick MD, Singleton ST, Vargas F, Kuo HC, et al. DMT-1: which metals does it transport? Biol Res 2006;39:79–85.
[16] Liuzzi JP, Aydemir F, Nam H, Knutson MD, Cousins RJ. *Zip14* (Slc39a14) mediates non-transferrin-bound iron uptake into cells. Proc Natl Acad Sci (USA) 2006;103: 13612–7.
[17] Peters JL, Dufner-Beattie J, Xu W, Geiser J, et al. Targeting the mouse Slc39a2 (*Zip2*) gene reveals highly cell specific patterns of expression and unique functions in zinc, iron and calcium homeostasis. Genesis 2007;45:339–52.
[18] Iyengar V, Pullakhandam R, Nair KM. Iron–zinc interaction during uptake in human intestinal Caco-2 cell line: kinetic analyses and possible mechanism. Ind J Biochem Biophys 2009;46:299–306.
[19] Laemmli UK. Cleavage of structural proteins during assembly of the head of bacteriophage T4. Nature 1970;227:680–5.
[20] Campanella A, Levi S, Cairo G, Biasiotto G, Arosio P. Blotting analysis of native IRP1: a novel approach to distinguish the different forms of IRP1 in cells and tissues. Biochemistry 2004;43:195–204.
[21] Yasunobu A, Suzuki KT. Detection of metallothionein by western blotting. Methods Enzymol 1991;205:108–14.
[22] Kilari S, Raghu P, Nair KM. Zinc inhibits oxidative stress induced iron signaling and apoptosis in Caco-2 cells. Free Radic Biol Med 2010;48:961–8.
[23] Bejjani S, Pullakhandam R, Punjal R, Nair KM. Gastric digestion of pea ferritin and modulation of its iron bioavailability by ascorbic and phytic acids in Caco-2 cells. World. J Gastroenterol 2007;13:2083–8.
[24] Barisani D, Parafioriti A, Bardela MT, Zoller H, Conte D, Armiraglio E, et al. Adaptive changes of duodenal transport proteins in Coeliac disease. Physiol Genomics 2004;17:316–25.
[25] Zoller H, Koch RO, Theurl I, Obrist P, Pietrangelo A, et al. Expression of the duodenal iron transporters divalent-metal transporter 1 and ferroportin 1 in iron deficiency and iron overload. Gastroenterology 2001;120:1412–9.
[26] Sreedhar B, Nair KM. Iron dependence and zinc inhibition of duodenal cytosolic aconitase of rat. Ind J Biochem Biophys 2004;41:250–3.
[27] Bobo JA. Characterization of zinc transporters in Caco-2 cells. Thesis presented to the University of Florida, Florida. 2004. url- http://etd.fcla.edu/UF/UFE0007019/bobo_j.pdf.
[28] Dufner-Beattie J, Wang F, Kuo YM, Gitschier J, Eide D, Andrews GK. The acrodermatitis enteropathica gene *ZIP4* encodes a tissue-specific, zinc-regulated zinc transporter in mice. J Biol Chem 2003;278(35):33474–81.
[29] Beyersmann D, Hasse H. Functions of zinc in signaling, proliferation and differentiation of mammalian cells. Biometals 2001;14:331–41.
[30] Murgia C, Vespignani I, Cerase J, Nobili F, Perozzi G. Cloning, expression and vesicular localization of zinc transporter Dri27/ZnT4 in intestinal tissue and cells. Am J Physiol 1999;277:G1231–1239.
[31] Maclean KH, Cleveland JL, Porter JB. Cellular zinc is a major determinant of iron chelator-induced apoptosis of thymocytes. Blood 2001;98:3831–9.
[32] Liuzzi JP, Cousins RJ. Mammalian zinc transporters. Ann Rev Nutr 2004;24: 151–72.
[33] Liuzzi JP, Bobo JA, Cui L, McMahon RJ, Cousins RJ. Zinc transporters 1, 2 and 4 are differentially expressed and localized in rats during pregnancy and lactation. J Nutr 2003;133(2):342–51.
[34] Palmiter RD, Huang L. Efflux and compartmentalization of zinc by members of the SLC30 family of solute carriers. Pflugers Arch 2004;447(5):744–51.